Modern Physics Letters A
Vol. 39, No. 3 (2024) 2350192 (10 pages)

DOI: 10.1142/S0217732323501924

Time behavior of hubble parameter by torsion

Klaus Morawetz

Münster University of Applied Sciences,
Stegerwaldstrasse 39, 48565 Steinfurt, Germany

International Institute of Physics - UFRN,
Campus Universitário Lagoa nova,
59078-970 Natal, Brazil
morawetz@fh-muenster.de

Received 28 August 2023
Revised 23 November 2023
Accepted 11 December 2023
Published 3 February 2024

Consequences of the consistent exact solution of Einstein–Cartan equation on the time dependence of Hubble parameter are discussed. The torsion leads to a space and time-dependent expansion parameter which results into nontrivial windows of Hubble parameter between diverging behavior. Only one window shows a period of decreasing followed by increasing time dependence. Provided a known cosmological constant and the present values of Hubble and deceleration parameter this changing time can be given in the past as well as the ending time of the windows or universe. The comparison with the present experimental data allows to determine all parameters of the model. Large-scale spatial periodic structures appear. From the metric with torsion outside matter, it is seen that torsion can feign dark matter.

Keywords: Cosmology; torsion; Hubble-parameter.

PACS Nos.: 04.50.Kd, 98.80.Es, 98.80.-k

1. Introduction

There is an ongoing discrepancy of Hubble data from the early universe obtained by background radiation and data from present galaxies[1]: "We find a 5σ difference with the prediction of H_0 from Planck cosmic microwave background observations under λCDM, with no indication that the discrepancy arises from measurement uncertainties or analysis variations considered to date. The source of this now long-standing discrepancy between direct and cosmological routes to determining H_0 remains unknown." This discrepancy is also further supported by quasars at far distance.[2,3] This tension in H_0 is related to the anomaly in Ω_m of the Friedmann equations. H_0 decreases with effective redshift, while Ω_m increases with effective redshift in LCDM models.[4] This is attributed to negative dark energy density.[5] Obviously only in special models H_0 does not evolve.

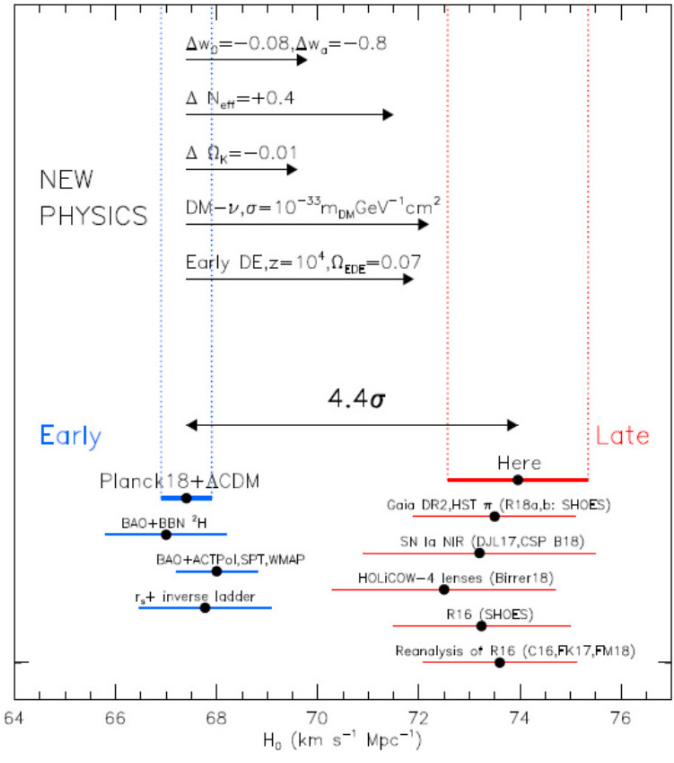

Fig. 1. The present data of Hubble constant from Ref. 6.

In Fig. 1, the data of the earlier paper are presented and obviously the discrepancy has increased now by 5σ.

Considering the time dependence of the scale parameter

$$R(t) = R_0(t_0)\Big[1 + H_0(t - t_0) - \frac{q}{2}H^2(t - t_0)^2 + \cdots\Big] \tag{1}$$

with the Hubble and deceleration parameters

$$H = \frac{\dot{R}}{R}, \quad q = -\frac{\ddot{R}R}{R^2}, \tag{2}$$

we adopt for the moment (2) as a literal definition which would lead to a time change of Hubble parameter

$$\dot{H} = \frac{\ddot{R}R - \dot{R}^2}{R^2}. \tag{3}$$

By demanding $\dot{H} > 0$ means $\ddot{R}R > \dot{R}^2$ and with the help of (2), one finds the equivalence

$$\dot{H} > 0 \leftrightarrow q < -1. \tag{4}$$

Consequently, the search is going on for such a negative deceleration parameter. An analysis of the Planck data and SHOES collaboration[7] indeed seems to indicate parameters

$$\begin{aligned} H_0 &= 75.35 \pm 1.68\,\mathrm{km/sMpc}, \\ q_0 &= -1.08 \pm 0.29. \end{aligned} \tag{5}$$

The theoretical challenge is how the Hubble parameter could increase with time.[8–10] One possible solution is provided by torsion leading to a metric due to an exact solution[11,12] of Einstein–Cartan equations. In the latter, the additional gravitational potential due to torsion becomes

$$U_{ik} = \frac{1}{2}\left[s_i^j s_{jk} + \sigma^2\left(u_i u_k + \frac{g_{ik}}{2}\right)\right] \tag{6}$$

in the Einstein–Cartan equations

$$G_{ik} = P_{ik} - \left(\lambda + \frac{P}{2}\right) g_{ik} = \kappa T_{ik} + \kappa\varepsilon Z_{ik} + \kappa^2 U_{ik}. \tag{7}$$

Here, we use $P = P_i^i$ and the cosmological constant λ. An additional part by torsion comes from the Belinfante–Rosenfeld equation[13,14] which relates the dynamical metric $\mathcal{T}$ and the canonical energy–momentum T tensor by

$$\begin{aligned} \mathcal{T}_{ik} &= T_{ik} + \varepsilon Z_{ik}, \\ Z_{ik} &= -\frac{1}{2}\nabla_l(s_k^l u_i + s_i^l u_k + s_{ki} u^l). \end{aligned} \tag{8}$$

This difference we indicate by a constant $\epsilon = 0$ or $\epsilon = 1$ dependent whether we use the metric variational principle or the torsion tensor as variation variable. The metric and torsion are dependent on each other even outside matter which consistency results into the antisymmetric spin tensor in terms of the Weyssenhoff spin liquid parameter $2\sigma^2 = s_l^m s_m^l$ with the only nonzero components in spherical coordinates[11]

$$s_{2,3}(t, r, \theta, \phi) = -s_{3,2} = \sigma r^2 \sin\theta. \tag{9}$$

Besides the Schwarzschild solution with zero torsion, it has been found that there exists exactly a second solution of these Eq. (7) outside matter with the metric[11]

$$ds^2 = \hat{r}^2 d\hat{t}^2 - \frac{3}{C + \lambda\hat{r}^2} d\hat{r}^2 - \hat{r}^2(d\theta^2 + \sin^2\theta d\hat{\phi}^2), \tag{10}$$

where we abbreviate

$$C = \frac{3(1+2\varepsilon)}{2(2+3\varepsilon)} = \begin{cases} 3/4, & \epsilon = 0, \\ 9/10, & \epsilon = 1. \end{cases} \tag{11}$$

A further transformation

$$\hat{r}^2 = \cos^2\tilde{t}\left[c(\tilde{r})^2 \tan^2\tilde{t} - 1\right], \quad \coth\hat{t} = c(\tilde{r})\tan\tilde{t} \tag{12}$$

with

$$c(\tilde{r}) = \tan\left(c + \sqrt{\frac{C}{3}}\ln\tilde{r}\right), \quad \tilde{r} = \sqrt{\frac{|\lambda|}{3}}r, \quad \tilde{t} = \sqrt{\frac{|\lambda|}{3}}t, \tag{13}$$

translates the metric (10) into a Friedman–Lamaître–Robertson–Walker metric

$$ds^2 = dt^2 - a(r,t)(dr^2 + r^2 d\Omega^2). \tag{14}$$

The expansion or scale parameter becomes now space and time-dependent

$$a(r,\tilde{t}) = R^2(r,t) = \frac{C\sin^2\sqrt{\frac{|\lambda|}{3}}t}{|\lambda|r^2\cos^2\left(2c + \sqrt{\frac{C}{3}}\ln\sqrt{\frac{|\lambda|}{3}}r\right)} \tag{15}$$

with an arbitrary constant c. It provides a time-like universe for $\tilde{r}^2 < \coth^2\tilde{t} - 1$ and a space-like otherwise.

2. Time Dependence of Hubble Parameter

2.1. *Local simplistic picture*

From the seemingly factorization of time and space dependence in the expansion parameter (15), one might be tempted to calculate locally the Hubble constant H and the delay parameter q directly via (2) as

$$H(t) = \frac{\dot{R}}{R} = \sqrt{\frac{|\Lambda|}{3}}\cot\sqrt{\frac{|\Lambda|}{3}}t, \tag{16}$$

$$q(t) = -\frac{R\ddot{R}}{\dot{R}^2} = \tan^2\sqrt{\frac{|\Lambda|}{3}}t = \frac{\lambda}{3H^2(t)}, \tag{17}$$

which divides out the spatial dependence which is too simplistic and will lead to a wrong behavior. This result is plotted in Fig. 2. We see that we have only a

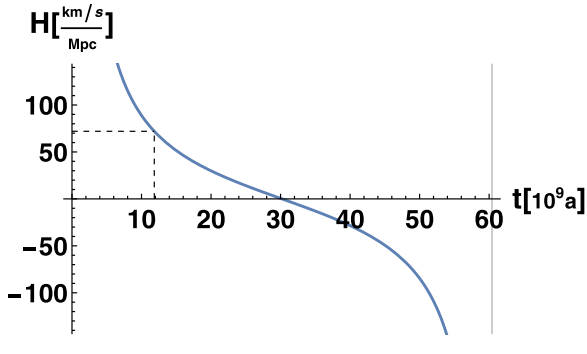

Fig. 2. Simplistic (locally fixed) time dependence of Hubble constant (17) leading to the wrong time dependence. Zero time is set at vanishing Hubble constant and the present is indicated by dashed lines.

time-decreasing Hubble parameter with $q_0 > 0$ in contrast to the data above. The reason is that the light coming from the past is running on $r = r_0 + c(t - t_0)$ and we cannot just simply divide out the spatial dependence. This we will consider more closely in the following section.

First, let us see to what values the local assumption (17) will lead which might explain a discrepancy to earlier data. We assume that the starting time t_0 is fixed at $H(t_0) = 0$. Then the Hubble constant at present time $H_0 = H(t_p)$ and q_0 is related with the cosmological constant as

$$\lambda = 3q_0 H_0^2 \sim H_0^2, \tag{18}$$

which is in agreement of high-redshift rotation curves and MOND calculations.[15] Within this simplistic picture, we assume the older value $q_0 \approx 1/2$ and see from (17) that the initial time is $t_0 = 0$ for $H = \infty$, the present and final time where the Hubble constant vanishes read

$$\begin{aligned} t_p &= \frac{1}{\sqrt{q_0} H_0}(\pi - \operatorname{arccot}\sqrt{q_0}) - t_0 \approx 11.8 \times 10^9 \mathrm{a}, \\ t_\infty &= \frac{\pi}{\sqrt{q_0} H_0} - t_0 \approx 30.2 \times 10^9 \mathrm{a}, \end{aligned} \tag{19}$$

respectively, with $1/H_0 \approx 13.6 \times 10^9 \mathrm{a}$.

The relative time change of the Hubble constant plotted in Fig. 2 in this simplistic picture would be at present $\dot{H}/H(t_0) \approx -2 \times 10^{-10} \mathrm{a}^{-1}$. All these times agree astonishingly well with the Big Bang scenario though only locally measured and with the wrong time dependence. We will see that these values changes only slightly if we consider correctly the time the light travels from far distances which will lead to the right time dependence of accelerating Hubble parameter. The wrong time dependence of the Hubble parameter here in local approximation has followed only from the structure of the metric and the cosmological constant and is independent of the factor C describing the spatial dependence of the expansion parameter. This problem in late-time cosmology are typical for models like Lambda cold dark matter (ΛCDM). Extensions lead to models with an extra parameter,[16] or e.g. investigation of unparticle cosmology.[17]

2.2. *Hubble parameter from distant light*

The spatial and time dependence of the expansion parameter (15) allows to consider the time the light is traveling from far distances. In Fig. 3, we plot the square of this expansion parameter as a function of time and space. Contrary to the simplistic picture before we measure light from distant objects. This means we cannot consider space and time independently as before. Instead, we have to consider Hubble parameter at the light path $r = r_0 + c(t - t_0)$ indicated by the red line in Fig. 3. One sees the oscillating behavior with respect to space and time. The spatial variation shows interestingly one additional maxim at large distances before it falls off rapidly.

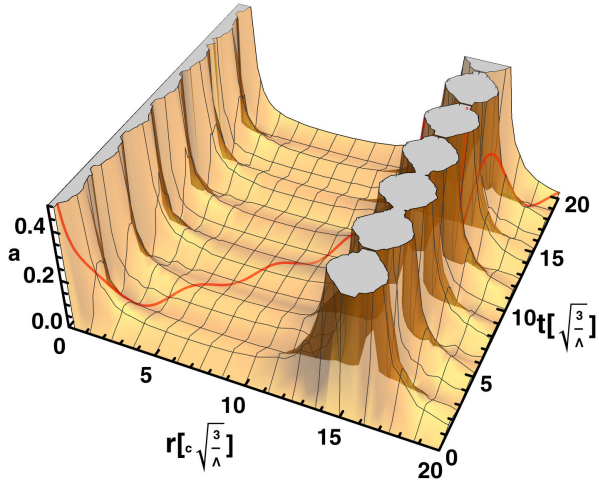

Fig. 3. (Color online) The time and space dependence of the expansion parameter (15) with the light path $r = r_0 + c(t - t_0)$ (red).

Working in dimensionless values

$$H = \sqrt{\frac{\lambda}{3}}\, h, \quad \bar{r} = \sqrt{\frac{\lambda}{3c^2}}\, r, \quad \tau = \sqrt{\frac{\lambda}{3}}\, t \tag{20}$$

with speed of light c we obtain with time derivatives along the light path the time-dependent Hubble and deceleration parameter

$$\begin{aligned} h(\tau) &= \cot\tau + \frac{\sqrt{\frac{C}{3}}\tan\sqrt{\frac{C}{3}}\ln(\bar{r}_0+\tau) - \sqrt{3}}{\bar{r}_0+\tau}, \\ q(\tau) &= -1 + \frac{1}{h(\bar{r}_0+t)} + \frac{(\bar{r}_0+t)\csc^2 t - \cot t}{h^2(\bar{r}_0+t)} - \frac{C\sec^2\left(\sqrt{\frac{C}{3}}\log(\bar{r}_0+t)\right)}{3h^2(\bar{r}_0+t)^2}. \end{aligned} \tag{21}$$

In Fig. 4, we see that the periodic oscillation along the light cone reveals only one certain window where the Hubble parameter can increase with time $\dot{H} > 0$ as observed. By choosing this interval as indicated by the shaded area, we can determine the initial and final time of this universe window as the present cosmos by $H(t_0) = H(t_\infty) = \infty$, the present time by $H(t_p)$ and the time where the Hubble parameter changes from falling to increasing time by $\dot{H}(t_c) = 0$. We determine the present time by reproducing the deceleration parameter (21) according to the value (5). For any parameter r_0, we can now determine these times together with the cosmological constant plotted in Fig. 5.

We see that the unknown parameter $\bar{r}_0$ as the starting place in Fig. 3 determines all three values of initial time, ending time as well as the cosmological constant due to the known present data (5). Larger $\bar{r}_0$ implies larger times accompanied by larger cosmological constant. In turn, if we know the cosmological constant by other

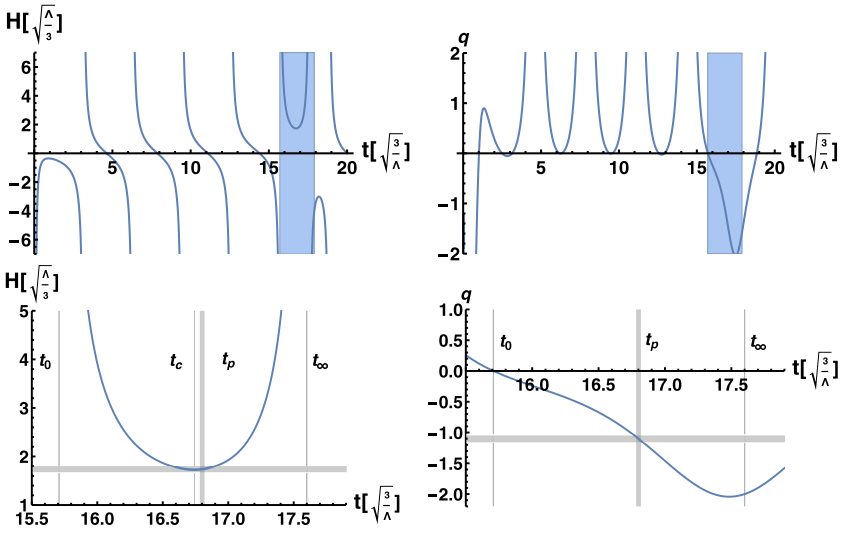

Fig. 4. The dimensionless Hubble parameter (left) and deceleration parameter (right) as function of dimensionless time assuming a present position of $r_0 = 0$. Below a zoom of the only possible window with $\dot{h} > 0$ indicated by shaded area. The present values at $t = t_p$ according to (5) are indicated by thick grid-lines.

measurements we know $\bar{r}_0$ and the times are fixed. Note that we have set the timescale to initially $t_0 = 0$ such that only the differences in times matter. The oscillating behavior as big bounce instead of big bang has been reported in Refs. 18 and 19 due to torsion. Such turning point in the Hubble parameter was obtained by

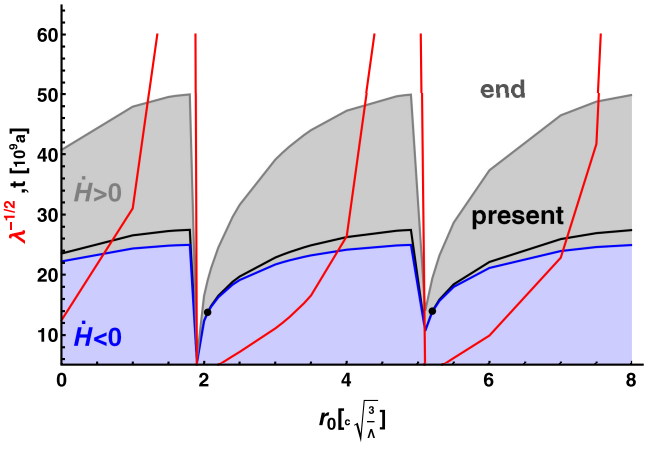

Fig. 5. (Color online) The age of present universe together with the age where the Hubble parameter changes from falling into increasing value vs. the dimensionless parameter of present location r_0. The data at presence are middle (black) lines and the corresponding cosmological constant are red lines. The best agreement with experimental data is indicated by dots outlines in Fig. 6.

considering unstable de Sitter state.[8] Depending on the parameter r_0, we can now find different ages and ending of the universe.

For a given r_0 parameter, we have the time dependence of Hubble parameter and deceleration parameter in (21) fixed according to (5). We can now compare with the experimental values which are given in terms of the red shift $z = -1 + R_0/R$. One has for the time dependence

$$\dot{z} = -\frac{R_0}{R}\frac{\dot{R}}{R} = (-1+z)H \tag{22}$$

and therefore with $z_0 = 0$ at present time t_0

$$z(t) = -1 + \exp\left[-\int_{t_0}^{t} d\bar{r} H(\bar{t})\right]. \tag{23}$$

Using the time as parameter, we can plot in Fig. 6 the Hubble parameter versus redshift keeping the present Hubble constant at the value of (5). The best choices of r_0 are indicated by dots in Fig. 5 according to the experimental data in Fig. 6. For further comparison of the data with present models, see Ref. 17. The resulting time where decelerating Hubble parameter changes into accelerating t_c, the present age t_p and the end of universe t_∞ read then

$$\begin{aligned}
&r_0 = 2.05\,(4.1\,\mathrm{Gpc}):\\
&t_c = 14.0413Ga, \quad t_0 = 14.1518Ga, \quad t_\infty = 19.5727Ga, \quad \lambda^{-1/2} = 3.78811Ga,\\
&r_0 = 5.2\,(10.7\,\mathrm{Gpc}):\\
&t_c = 14.2399Ga, \quad t_0 = 14.3581Ga, \quad t_\infty = 19.9614Ga, \quad \lambda^{-1/2} = 3.87425Ga.
\end{aligned} \tag{24}$$

In Fig. 5, one sees that almost similar realizations of experimental values are possible for periodically appearing r_0 where we have listed only the first two ones.

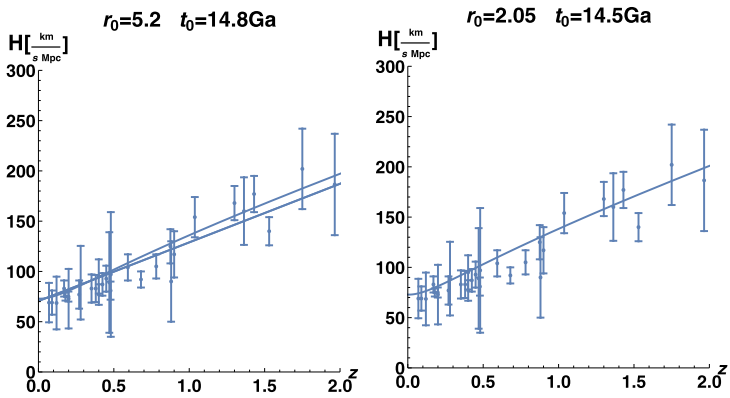

Fig. 6. The Hubble parameter vs. redshift together with the experimental data compilation of Ref. 20 for the best situation of Fig. 5.

3. Conclusion

A time dependence of the Hubble and deceleration parameter is found from the exact solution of Einstein–Cartan equations. The latter provides a spatial and time-dependent expansion or scale parameter. It is shown that the evolution of the universe is starting with an decreasing Hubble parameter switching to an increasing one within a certain evolution window among possible cosmoses. The seemingly dependence of the certain times and Hubble behavior on the position parameter r_0 is indicating a violation of equivalence principle. It appears here as an artificial unknown parameter for large-scale structures determined by the cosmological constant. Since the Einstein–Cartan equations complete the equivalence principle[21] or more recently[22] and since we have used an exact solution of the latter we can conclude that locally there exist a transformation to a frame where the gravitational force vanishes though the large scale time and space structure of the expansion parameter looks nonholonomic.

As a second hint, we should note that the torsion can mime dark matter. This can be seen as follows. We rewrite (10) into the Schwarzschild form:

$$ds^2 = \left(1 - \frac{a}{r}\right)dt^2 - \frac{1}{1 - \frac{b}{r}}dr^2 - r^2 d\Omega^2 \tag{25}$$

with

$$a = r - \frac{|\Lambda|}{3}r^3, \quad b = \left(1 - \frac{C}{3}\right)r - \frac{|\Lambda|}{3}r^3. \tag{26}$$

If we compare this result of the new metric with the standard Schwarzschild solution with zero torsion and the extension to include the cosmological constant known as Kottler solution[23]

$$a^K = 2M - \frac{|\Lambda|}{3}r^3, \quad b^K = 2M - \frac{|\Lambda|}{3}r^3, \tag{27}$$

we can conclude that the new metric resulting from torsion induces a mass like term

$$M^{\text{torr}} = \frac{1}{2}\left(1 - \frac{C}{3}\right)r, \tag{28}$$

which increases with larger distances. This can probably mime an additional gravitational mass[24] modifying the outer rotation of large galaxies.[25] Recent investigations for torsion leading to dark energy can be found in Ref. 26.

The found periodic spatial dependence r_0 in (24) agrees well with the recently observed large ring structures, see Refs. 27 and 28.

ORCID

Klaus Morawetz https://orcid.org/0000-0003-2119-9461

References

1. A. G. Riess, W. Yuan, L. M. Macri, D. Scolnic, D. Brout, S. Casertano, D. O. Jones, Y. Murakami, G. S. Anand, L. Breuval, T. G. Brink, A. V. Filippenko, S. Hoffmann, S. W. Jha, W. D. Kenworthy, J. Mackenty, B. E. Stahl and W. Zheng, *Astrophys. J. Lett.* **934**, L7 (2022).
2. R. G. and E. Lusso, *Nat. Astron.* **3**, 172 (2019).
3. X. Li, R. E. Keeley, A. Shafieloo, X. Zheng, S. Cao, M. Biesiada and Z.-H. Zhu, *Mon. Not. R. Astron. Soc.* **507**, 919 (2021).
4. E. Ó. Colgáin, M. M. Sheikh-Jabbari, R. Solomon, G. Bargiacchi, S. Capozziello, M. G. Dainotti and D. Stojkovic, *Phys. Rev. D* **106**, L041301 (2022).
5. M. Malekjani, R. M. Conville, E. Colgáin, S. Pourojaghi and M. M. Sheikh-Jabbari, Negative dark energy density from high redshift pantheon+ supernovae (2023), arXiv:2301.12725 [astro-ph].
6. A. G. Riess, S. Casertano, W. Yuan, L. M. Macri and D. Scolnic, *Astrophys. J.* **876**, 85 (2019).
7. D. Camarena and V. Marra, *Phys. Rev. Res.* **2**, 013028 (2020).
8. E. O. Colgáin, M. H. van Putten and H. Yavartanoo, *Phys. Lett. B* **793**, 126 (2019).
9. W.-M. Dai, Y.-Z. Ma and H.-J. He, *Phys. Rev. D* **102**, 121302 (2020).
10. E. Colgáin and M. M. Sheikh-Jabbari, *Class. Quantum Grav.* **38**, 177001 (2021).
11. K. Morawetz, *Class. Quantum Grav.* **38**, 205003 (2021).
12. Errata, *Class. Quantum Grav.* **40**, 029501 (2022).
13. F. Belinfante, *Physica* **7**, 449 (1940).
14. L. Rosenfeld, *Sur le tenseur d'impulsion-énergie* (Palais des Académies, 1940), impr. de G. Thone.
15. M. Milgrom, High-redshift rotation curves and MOND (2017).
16. A. Maeder, *Astrophys. J.* **834**, 194 (2017).
17. M. A. Abchouyeh and M. H. P. M. van Putten, *Phys. Rev. D* **104**, 083511 (2021).
18. N. J. Popławski, *Phys. Lett. B* **694**, 181 (2010).
19. N. Popławski, *Phys. Rev. D* **85**, 107502 (2012).
20. J. Ryan, S. Doshi and B. Ratra, *Mon. Not. R. Astron. Soc.* **480**, 759 (2018).
21. P. Von Der Heyde, *Lett. Nuovo Cimento* **14**, 250 (1975).
22. G. Pradisi and A. Salvio, *Eur. Phys. J. C* **82**, 840 (2022).
23. X. Chongming, W. Xuejun and H. Zhun, *Gen. Relat. Gravit.* **19**, 1203 (1987).
24. N. J. Popławski, *Phys. Rev. D* **83**, 084033 (2011).
25. A. L. González-Morán, R. Chávez, E. Terlevich, R. Terlevich, D. Fernández-Arenas, F. Bresolin, M. Plionis, J. Melnick, S. Basilakos and E. Telles, *Mon. Not. R. Astron. Soc.* **505**, 1441 (2021).
26. D. Benisty, E. Guendelman and H. Stoecker, *Eur. Phys. J.* **82**, 264 (2022).
27. A. M. Lopez, R. G. Clowes and G. M. Williger, *Mon. Notices Royal Astron. Soc.* **516**, 1557 (2022).
28. P. K. Aluri, P. Cea, P. Chingangbam, M.-C. Chu, R. G. Clowes, D. Hutsemekers, J. P. Kochappan, A. M. Lopez, L. Liu, N. C. M. Martens, C. J. A. P. Martins, K. Migkas, E. O. Colgain, P. Pranav, L. Shamir, A. K. Singal, M. M. Sheikh-Jabbari, J. Wagner, S.-J. Wang, D. L. Wiltshire, S. Yeung, L. Yin and W. Zhao, *Class. Quantum Grav.* **40**, 094001 (2023).